

7.6. Barrow, Alaska

UV data from Barrow differ from the austral high latitude sites in several ways. For example, the “ozone-sensitive” data products, particularly biologically effective dose-rates and the integral around 300 nm, show much smaller short-term variability than at the austral sites due to less severe ozone depletion in the Arctic.

In Figure 7.6.1, recent column ozone data from the Ozone Monitoring Instrument (OMI) onboard NASA’s AURA satellite are compared with ozone records from the years 1991-2012. There is a strong seasonal dependence: ozone columns are generally higher and have a larger variability during spring than autumn. Measurements in 2013 were continuously below the long-term mean between 3 and 18 March and above the mean between 28 April and 20 May, with two exceptions (9 and 10 May). Another period with above-average ozone occurred between 29 May and 9 June.

The daily maximum UV index (Figure 7.6.2) was suppressed between 1 May and mid-June 2013. This may have three reasons: the relative high ozone column between 1 May and 20 May, the rapid drop in surface albedo between 25 May and 20 June, and higher-than-normal cloudiness. Relatively low UV values during this period were also observed for other data products such as the spectral irradiance integrated over 298.51 - 303.03 nm (Figure 7.6.3), DNA-weighted daily dose (Figure 7.6.4), and erythemally-weighted daily dose (Figure 7.6.5), respectively.

Daily irradiation in the 400-600 nm band is shown in Figure 7.6.6. Visible radiation is virtually not affected by the ozone column and changes in surface albedo have a smaller effect compared to wavelengths in the UV. Measurements up to 19 May therefore agree reasonably well with historical data. However, also data in the visible are unusually low between 23 May and 10 June (the period immediately before the site visit). Higher-than-normal cloudiness is the likely reason. In general, radiation levels at all wavelengths are much more affected by clouds during summer and autumn than during spring, because high albedo in spring resulting from snow cover reduces cloud effects.

Factors affecting the annual cycles in UV and visible radiation at Barrow have been analyzed in great detail (Bernhard *et al.*, 2007). The annual ozone cycle was found to be the dominant parameter modifying UV-B irradiance, but the combined effects of albedo and clouds compensate for most of the ozone influence. High surface albedo caused by snow cover may increase UV irradiance by up to 57%. Aerosols lead to reductions of 5% typically, but larger reduction was observed during Arctic haze events, particularly during spring. For erythral irradiance, and measurements in the UV-A and visible, annual cycles of albedo and clouds are responsible for a pronounced seasonal asymmetry.

An example of the different characteristics of DNA-damaging and visible radiation is shown in Figure 7.6.7. Daily irradiation in the 400-600 nm spectral range is not centered at the summer solstice but shifted by about 15 days towards spring. The DNA curve on the other hand is nearly symmetrical with respect to the solstice. The reason for this distinct difference can be explained as follows: surface albedo is larger and clouds are less prevalent in spring than in autumn. This enhances radiation levels in spring and is the reason of the apparent shift of measurements in the visible. Higher albedo and less cloudiness also leads to larger DNA-damaging radiation, but the larger total ozone column in spring (Figure 7.6.1) compensates the enhancement. As a consequence, DNA-damaging radiation is of similar magnitude in spring and autumn.

Reference:

Bernhard, G., C. R. Booth, J. C. Ebrahimian, R. Stone, and E. G. Dutton (2007), Ultraviolet and visible radiation at Barrow, Alaska: Climatology and influencing factors on the basis of version 2 National Science Foundation network data, *J. Geophys. Res.*, 112, D09101, doi:10.1029/2006JD007865.

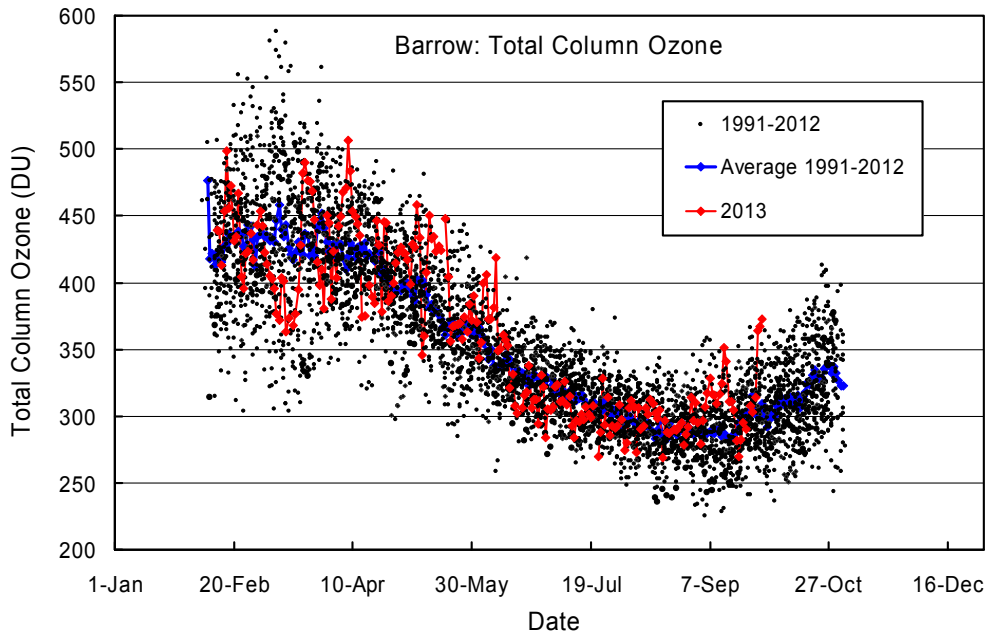


Figure 7.6.1. Total column ozone at Barrow. OMI measurements from 2013 are contrasted with ozone data from prior years recorded by TOMS on Nimbus-7 (1991-1993), Earth Probe (1996-2004), and OMI (2005-2012) satellites. TOMS data are from the Version 8 data set.

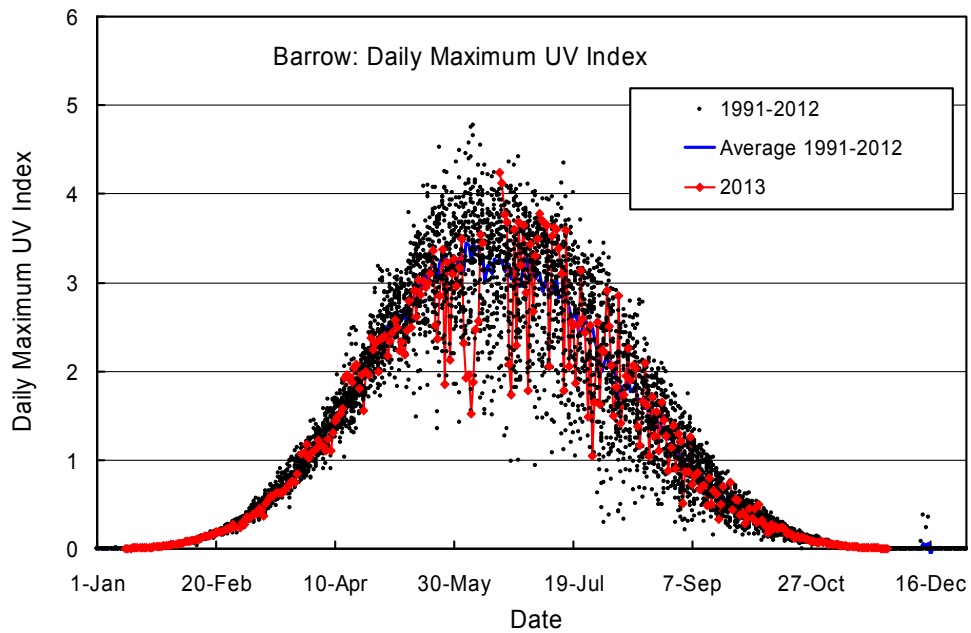


Figure 7.6.2. Daily maximum UV Index at Barrow. Measurements from 2013 are contrasted with individual data points and the average of measurements taken between 1991 and 2012.

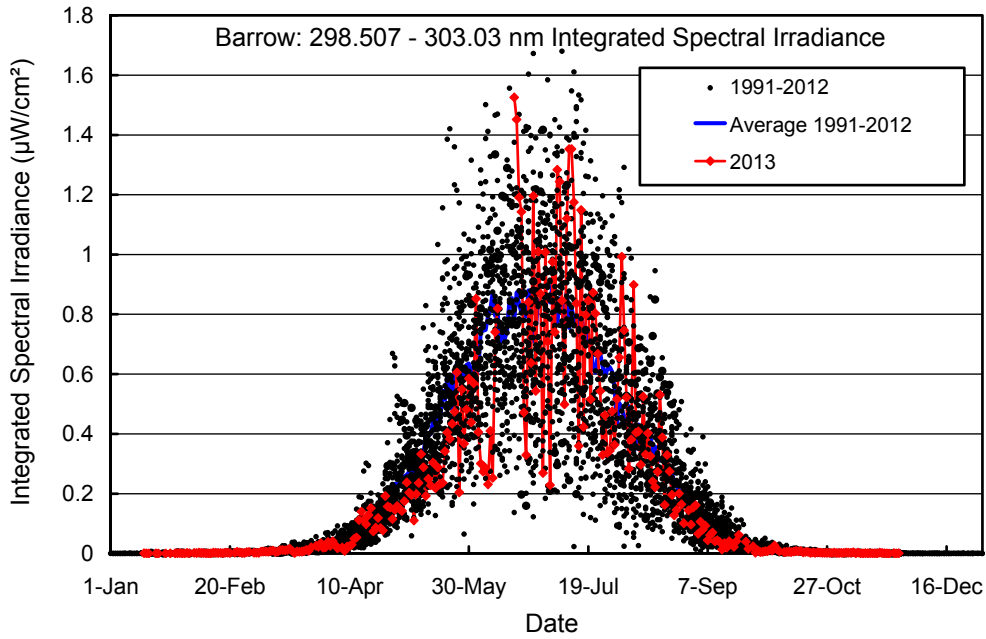


Figure 7.6.3. Noontime integrated spectral UV irradiance (298.51 - 303.03 nm) at Barrow. Measurements from 2013 are contrasted with individual data points and the average of measurements taken between 1991 and 2012.

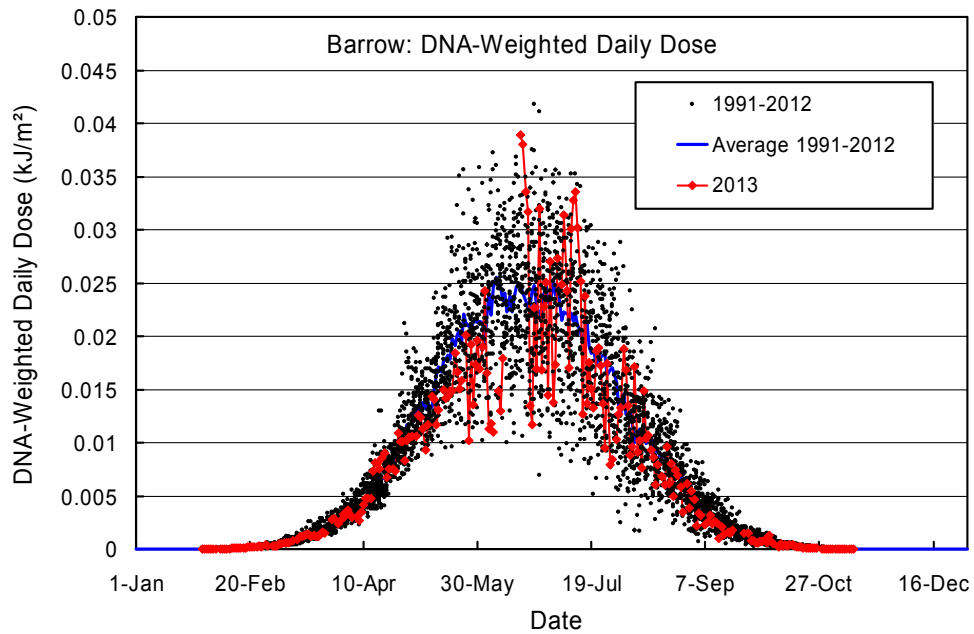


Figure 7.6.4. Daily DNA-weighted dose at Barrow. Volume 23 measurements from 2013 are contrasted with individual data points and the average of measurements taken between 1991 and 2012.

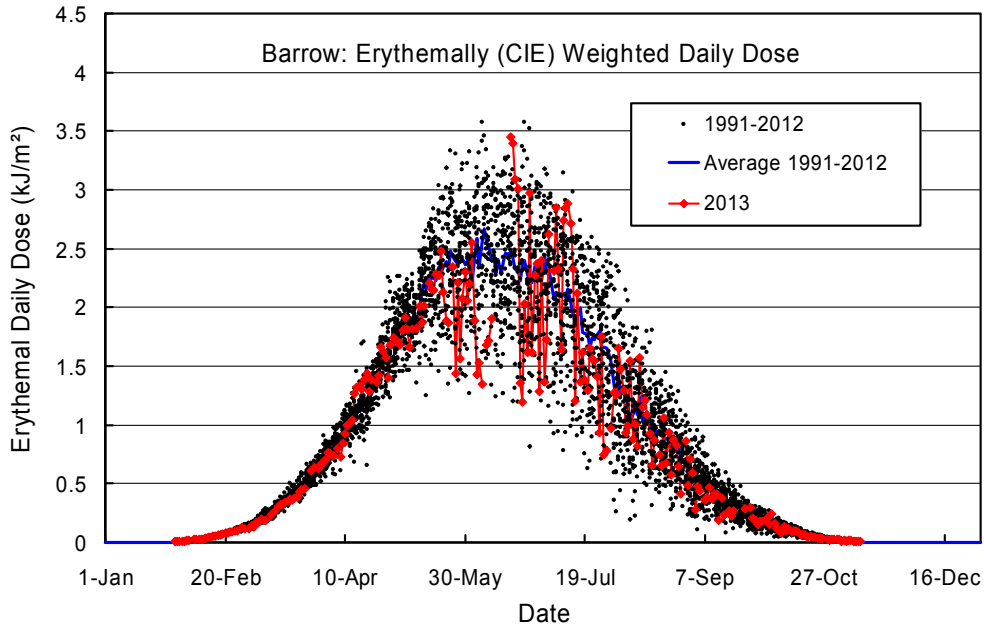


Figure 7.6.5. Daily erythemal dose at Barrow. Volume 23 measurements from 2013 are contrasted with individual data points and the average of measurements taken between 1991 and 2012.

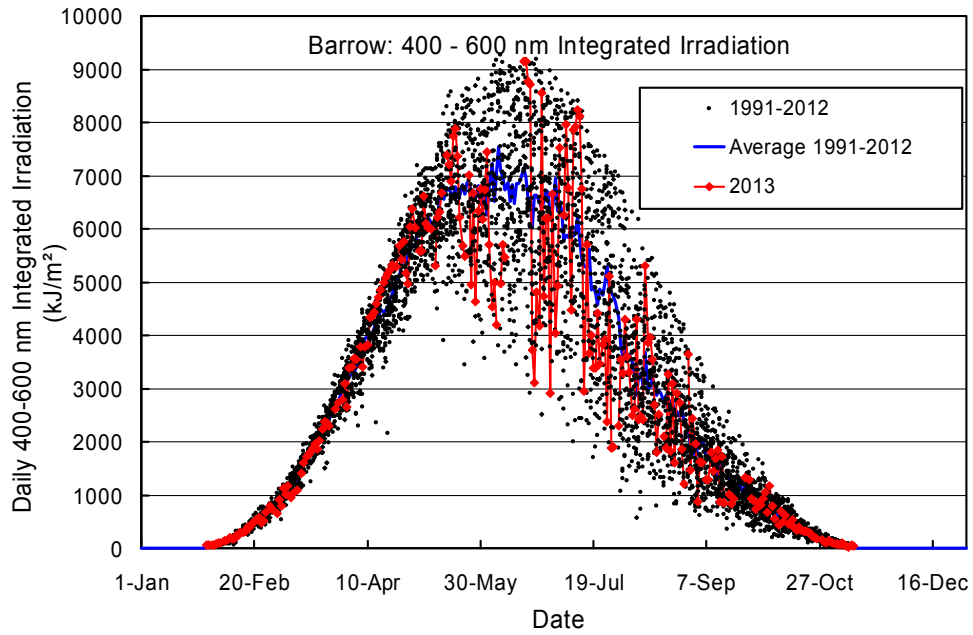


Figure 7.6.6. Daily irradiation of the 400-600 nm band at Barrow. Volume 23 measurements from 2013 are contrasted with individual data points and the average of measurements taken between 1991 and 2012.

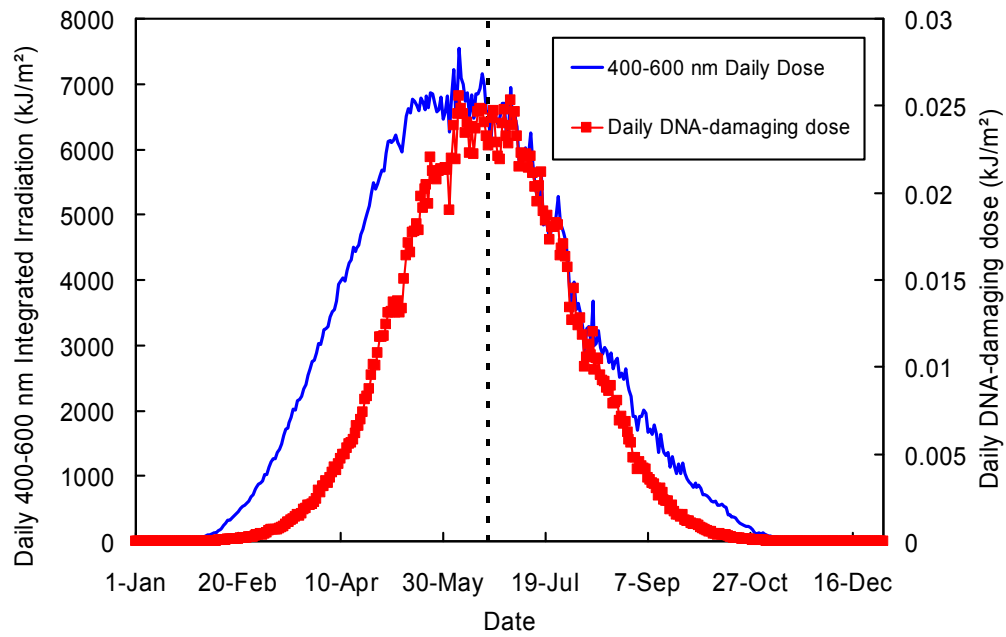


Figure 7.6.7. Comparison of DNA-weighted dose (right axis) with daily irradiation in the 400-600 nm spectral range (left axis) at Barrow. Both curves are average values for the period 1991-2012.